



Published in final edited form as:

Neurology. 2007 September 18; 69(12): 1245–1253. doi:10.1212/01.wnl.0000276947.59704.cf.

Clinical characterization of the HOXA1 syndrome BSAS variant

T.M. Bosley, MD, M.A. Salih, MD, I.A. Alorainy, MD, D.T. Oystreck, OC(C), M. Nester, PhD, K.K. Abu-Amero, PhD, M.A. Tischfield, BA, and E.C. Engle, MD

Neuro-ophthalmology Division (T.M.B., D.T.O.), King Khaled Eye Specialist Hospital; Division of Pediatric Neurology (M.A.S.) and Department of Radiology (I.A.A.), King Khalid University Hospital, King Saud University; Departments of Neuroscience (T.M.B., M.N.) and Genetics (K.K.A.-A.), King Faisal Specialist Hospital and Research Centre, Riyadh, Saudi Arabia; and the Program in Genomics, Children's Hospital Boston, and Program in Neuroscience (M.A.T., E.C.E.), Harvard Medical School, Boston, MA. Dr. Bosley is now with the Neurology Division, Cooper University Hospital, Camden, NJ; and Dr. Abu-Amero is now with the Shafallah Genetics Medical Center, Doha, Qatar.

Abstract

Background: The Bosley-Salih-Alorainy syndrome (BSAS) variant of the congenital human *HOXA1* syndrome results from autosomal recessive truncating *HOXA1* mutations. We describe the currently recognized spectrum of ocular motility, inner ear malformations, cerebrovascular anomalies, and cognitive function.

Methods: We examined nine affected individuals from five consanguineous Saudi Arabian families, all of whom harbored the same I75-I76insG homozygous mutation in the *HOXA1* gene. Patients underwent complete neurologic, neuro-ophthalmologic, orthoptic, and neuropsychological examinations. Six individuals had CT, and six had MRI of the head.

Results: All nine individuals had bilateral Duane retraction syndrome (DRS) type 3, but extent of abduction and adduction varied between eyes and individuals. Eight patients were deaf with the common cavity deformity of the inner ear, while one patient had normal hearing and skull base development. Six had delayed motor milestones, and two had cognitive and behavioral abnormalities meeting Diagnostic and Statistical Manual of Mental Disorders-IV criteria for autism spectrum disorder. MRI of the orbits, extraocular muscles, brainstem, and supratentorial brain appeared normal. All six appropriately studied patients had cerebrovascular malformations ranging from unilateral internal carotid artery hypoplasia to bilateral agenesis.

Conclusions: This report extends the Bosley-Salih-Alorainy syndrome phenotype and documents the clinical variability resulting from identical *HOXA1* mutations within an isolated ethnic population. Similarities between this syndrome and thalidomide embryopathy suggest that the teratogenic effects of early thalidomide exposure in humans may be due to interaction with the HOX cascade.

We recently reported a new Mendelian syndrome associated with truncating mutations in *HOXA1*, 1 a homeodomain transcription factor critical for the proper development of hindbrain rhombomeres in mice.^{2,3} Homozygous 175-176insG guanine base-pair insertions were found

Copyright © 2007 by AAN Enterprises, Inc. All rights reserved.

Address correspondence and reprint requests to Dr. Thomas M. Bosley, Cooper University Hospital, 3 Cooper Plaza, Suite 320, Camden, NJ 08103 Bosley-Thomas@cooperhealth.edu or Dr. Elizabeth C. Engle, Children's Hospital Boston, Program in Genomics, Enders 560.2, 300 Longwood Ave., Boston, MA 02115 elizabeth.Engle@childrens.harvard.edu.

Supplemental data at www.neurology.org

Disclosure: The authors report no conflicts of interest.

in several families from Saudi Arabia, while a homozygous 84C>G nonsense mutation resulted in the substitution of a stop codon for a tyrosine residue (Y28X) in a Turkish individual. These two mutations cause a phenotype, referred to as the Bosley-Salih-Alorainy syndrome (BSAS; OMIM #601536), characterized by bilateral Duane retraction syndrome (DRS) type 3, deafness, malformations of the cerebral vasculature, and autism in some patients.

We also identified a third mutation in exon 1 of *HOXA1*, a homozygous 76C>T change resulting in the substitution of a stop codon for an arginine residue (R26X), in Native American children with the previously reported Athabascan brainstem dysgenesis syndrome (ABDS; OMIM #601536).¹⁻⁴ These children share horizontal gaze restriction, deafness, and internal carotid artery (ICA) abnormalities with BSAS but also have central hypoventilation, facial and bulbar weakness, conotruncal heart defects, and mental retardation.

We now provide a more detailed clinical report of nine Saudi Arabian patients who harbor the same *HOXA1* mutation in order to elucidate the phenotypic variability of BSAS and its relationship to ABDS. An abbreviated phenotypic description of eight of these patients was provided in the original BSAS report.¹ The BSAS phenotype has implications for human brainstem development, for the etiology and variability of DRS, and for certain other congenital ocular motility syndromes and embryopathies.

METHODS

Patients

Nine affected individuals from five families were examined in neuro-ophthalmology clinics of the King Khaled Eye Specialist Hospital and the King Faisal Specialist Hospital and Research Centre and in the Pediatric Neurology Clinic of the King Khalid University Hospital in Riyadh, Saudi Arabia. The genetic features of eight of the individuals (Patients 1 through 8) were reported previously,¹ while Patient 9 was the child of an unrelated consanguineous family. She was genotyped more recently, using the same primer sequences and PCR conditions detailed previously, and was found to have the same homozygous *HOXA1* guanine insertion (I75-I76insG) founder mutation as other reported Saudi individuals. All families signed informed consent at the appropriate institution.

Clinical evaluation

All patients had complete neurologic, neuro-ophthalmologic, and orthoptic examinations, including videotaping of eye movements in eight individuals. Ocular motility and alignment was evaluated in all positions of gaze. Fusional status was evaluated using a variety of binocular vision tests including the Worth 4 Dot test, Titmus stereo-acuity test, Bagolini striated lenses, and ability to overcome base-out prism with convergence. Best-corrected visual acuity was assessed with methods appropriate for age and cognitive ability. All patients had dilated fundoscopic examinations.

Neuropsychological evaluation

Eight members of four Saudi families were seen by a neuropsychologist (M.N.), seven of whom were evaluated with the Vineland Adaptive Behavior (VAB) scale. VAB was administered by an experienced native neuropsychological technician trained in its use, and scoring for age equivalency was done independently by the neuropsychologist. All children other than the youngest (Patient 9) had repeated neurodevelopmental evaluations over several years (M.A.S.), and Diagnostic and Statistical Manual of Mental Disorders (DSM)-4 criteria for autism were applied separately by a neuropsychologist and a pediatrician. Patient 3 was also evaluated with the Childhood Autism Rating Scale (CARS).

Neuroimaging

Six affected individuals had MR images of the brain or neck. Standard brain MR pulse sequences were acquired in five patients using a 1.5 Tesla GE Signa scanner (GE Medical Systems, Waukesha, WI) or 1.5 Tesla Siemens Magnetom Vision (Siemens Medical Systems, Germany) including sagittal T1-weighted spin echo (350 to 500/10 to 15/1 [TR/TE/NEX]), coronal fluid-attenuated inversion recovery (8,800/130, inversion time, 2,200 msec), and axial dual echo (3,500/119 and 17). MR images were obtained in one patient on a 3.0 Tesla Siemens Magnetom Allegra scanner (Siemens Medical Systems) including sagittal T1-weighted (624/7), axial fluid-attenuated inversion recovery (8,000/80, inversion time 2400 msec), and axial MP-RAGE (2,500/4.4, 1 mm thickness) through the brain, and axial 3D FT constructive interference in steady-state of the inner ear and cerebellopontine angle (11/5.6, 1 mm thickness).

MR angiogram (MRA) of the head was obtained in five patients using time-of-flight (TOF) sequence and of the neck in four of them using TOF or phase contrast sequence. One patient had CT of the brain (7 mm slice thickness), and five had CT of the temporal bone (1 mm slice thickness). Volume data from CT were used for reconstruction of coronal petrous bone images.

RESULTS

Clinical and neuropsychological observations

Patient numbers for Patients 1 through 8 correspond to Supplementary Table 1 Online of Tischfield et al.,¹ while Patient 9 was proven more recently to have the same Saudi BSAS mutation. Table 1 includes basic demographics and certain general characteristics of these nine affected individuals (three male and six female, aged 3 to 20 years), while table E-1 (on the *Neurology* Web site at www.neurology.org) summarizes the developmental and cognitive characteristics of these patients, including the VAB scale.

Eight patients were deaf and mute while one had normal hearing and speech development. Eight had a variety of behavioral (sleep disturbance, grimacing) and somatic (affecting face, ear, gastrointestinal tract, genitourinary system, and feet) abnormalities. Two deaf patients with speech abnormalities (Patients 1 and 9) and the one patient with normal hearing (Patient 8) had grossly normal neurodevelopmental histories and examinations except for ocular motility. Six patients had developmental motor delay by report (two on examination when young), typically not walking until the age of 3 years. No patient had scoliosis, inappropriately small stature, or cervical spine malformation, but as a group they had a somewhat large cranial circumference. Three families reported a total of seven miscarriages.

Patients 3 and 5 met DSM-4 criteria for autistic spectrum disorder by examination, family report, and VAB scores. Patient 3, who was institutionalized, scored 42 on CARS examination, falling in the moderate/severe autistic range. Both children exhibited profound linguistic delay with virtually nonexistent nonverbal communication skills, impaired social functioning, lack of eye contact, stereotypic hand movements, tactile avoidance, and obsessional features, such as compulsively arranging pictures and objects in the environment and persistent preoccupation with bright or shiny parts of objects. They had no reciprocal play, and their interests were narrow. Self-care skills were uniformly poor. Families of both autistic individuals reported sleep disturbance, although the older individual had improved with age. Patient 7 also had autistic features with stereotyped movements, excessive shyness, and complete lack of language; however, she had nonverbal communication and socialized in a fashion typical of a deaf child her age.

Ocular motility

All patients had a moderately severe or complete limitation of adduction and abduction bilaterally with full vertical gaze, as detailed in table 2 and illustrated in figure 1. Six patients (Patients 1, 2, 4, 6, 8, and 9) had globe retraction and palpebral fissure narrowing on adduction bilaterally diagnostic of DRS type 3 (figure 1, A through F). Patient 7 had retraction documented only unilaterally; however, horizontal motility restriction was present bilaterally, and her older sister had unequivocal globe retraction bilaterally. Globe retraction and fissure narrowing was not observed in either eye of Patients 3 and 5 (figure 1, G through I). These patients had severe restriction of horizontal eye movement, and autism interfered with their ability to cooperate with the examination. Both patients had at least one BSAS-affected sibling with obvious DRS type 3 bilaterally. Bilateral globe retraction was readily apparent upon convergence in the three patients with strong convergence (Patients 4, 8, and 9).

Five patients (Patients 3, 5, 7 through 9) were orthotropic in primary position at distance (figure 1, E and H), while four (Patients 1, 2, 4, and 6) had an esotropia in primary position (figure 1B). Patient 6 had an accommodative element to her esotropia, and she was the only patient who underwent strabismus surgery to correct the horizontal deviation. Two patients had low amplitude nystagmus that was horizontal pendular in one (Patient 5) and vertical pendular in another (Patient 6). Three patients (Patients 2, 4, and 6) developed a vertical deviation on attempted horizontal gaze.

Afferent functioning

Seven patients had normal visual acuity, ocular fundi, pupillary function, and visual fields. Patient 2 had 20/80 acuity bilaterally, possibly because of age and ability to cooperate. Three patients (Patients 6, 7, and 8) demonstrated fusion. Patient 6 had a monofixation syndrome with a tiny residual manifest deviation following early strabismus surgery, while Patient 7 had no manifest deviation in primary position, and Patient 8 required a small left face turn to maintain binocular alignment (figure 1E).

Neuroimaging

Table 3 details results of neuroimaging studies. No imaged patient had gross congenital brain anomalies or evidence of ischemia. Orbits and extraocular muscles appeared normal in all studies (figure E-1, A and B). Brainstem and 4th ventricle were normally developed (figure E-1, C and D), as were supratentorial structures. Patient 8 had a 3 Tesla scan with thin MR sections through the caudal pons. These images were degraded by a pulsation artifact anterior to the pons, but the exiting abducens cranial nerve (CN) could not be identified bilaterally (figure E-1, E through G) despite routine identification of these nerves on control images. Scout views of five of the six patients undergoing head CT allowed gross evaluation of the cervical spine, all of which appeared normal.

The skull base was normal only in Patient 8, who had normal inner ear anatomy (figure 2A) and normal hearing, while the eight patients with sensorineural deafness had malformations involving the inner ear and petrous bone. Four patients (Patients 4 through 7) had the common cavity deformity (CCD) replacing cochlea, semicircular canals, and vestibule bilaterally (figure 2, B through D) and two (Patients 1 and 3) had CCD on one side and complete absence of inner ear structures on the other side (figure 2E). Carotid canals were absent bilaterally in Patient 5 and unilaterally in Patients 4 and 6 (figure 2B). Internal auditory canal (IAC) was absent or severely narrowed in the six patients with inner ear malformation (figure 2E). The combination of profound inner ear maldevelopment with absent carotid canal sometimes yielded the appearance of a small petrous bone with patulous Meckel's caves (figure 2F).

All six patients with MR angiography or MR imaging had abnormalities of the internal carotid arteries. The left internal carotid artery (ICA) was hypoplastic in Patients 1 and 8 (figure 3A) and absent in Patients 4, 6, and 7 (figure 3B) where the left common carotid artery terminated into the external carotid artery. Four patients (Patients 1, 6, 7, and 8) with hypoplastic or absent left ICAs had a right common carotid artery bifurcation quite low in the neck, at about the C7 level (figure 3C). All six patients with ICA anomalies had an enlarged posterior communicating artery on the side of an absent or hypoplastic ICA (figure 3, B, D, and E). The ICAs were absent bilaterally in Patient 5, who had blood supply to the brain only through an enlarged vertebrobasilar system (figure 3, D and E). The intracranial portion of the left vertebral artery was duplicated in Patient 5 (figure 3F), while Patient 1 had duplication of the proximal half of the left vertebral artery.

DISCUSSION

This comprehensive phenotypic description of patients with genetically defined BSAS expands the original brief report¹ and complements the description of ABDS that was published prior to identification of the underlying *HOXA1* mutation.⁴ BSAS is characterized by variable DRS type 3 bilaterally, deafness with malformation of the inner ear, and abnormal development of cerebral vasculature. When patients are young or uncooperative or when individuals have atypical features such as severely restricted horizontal ocular motility or normal hearing, these *HOXA1* syndromes may be difficult to distinguish phenotypically from autosomal recessive horizontal gaze palsy and progressive scoliosis (HGPPS; OMIM 607313). Table E-2 compares BSAS with ABDS and HGPPS,^{5,6} emphasizing genetic, clinical, and neuroimaging features important to the diagnosis.

The BSAS phenotype is variable among these nine patients. Horizontal ocular motility, globe retraction, and convergence were different between eyes and individuals. One patient had normal hearing with normal inner ear anatomy, while eight were deaf with a severe abnormality of cochlear and semicircular canal development. All studied patients had abnormalities of cerebral vasculature, but each had a unique constellation of abnormalities. Patients had a spectrum of somatic defects, most commonly involving external ears or extremities. Delayed motor development could be explained by the lack of a vestibular system rather than by a generalized brain disturbance in most patients. However, two were unequivocally autistic and a third had a number of autistic features, implying an abnormality extending beyond the brainstem. Some of the variability between patients could be interpreted as a severity gradient, from relatively mild involvement (e.g., Patient 8 with modest ocular motility, normal hearing, only left ICA hypoplasia, and normal cognition) to more severe disease (e.g., Patient 5 with no observed horizontal eye movement, deafness and CCD bilaterally, absent ICA bilaterally, and autism).

These patients with BSAS are distinct among patients with inherited DRS⁷⁻¹² because they have bilateral DRS with limitations of both adduction and abduction. DRS is now understood as a neurogenic problem in which an abnormal abducens nerve results in a denervated lateral rectus muscle that is aberrantly innervated by the inferior division of the oculomotor nerve that also innervates the ipsilateral medial rectus muscle.¹³ This innervation pattern is believed to precipitate co-contraction of lateral and medial recti, causing the globe retraction and fissure narrowing on adduction and convergence that define DRS.^{14,15} Abducens nucleus interneurons are spared in unilateral DRS type 1,^{13,16} where the contralateral eye moves normally, but their status is uncertain in bilateral DRS type 3.

Given that the abducens cranial nerve is absent in the *Hoxa1*^{-/-} mouse model¹⁷ and probably also in one patient reported here, it seems likely that both BSAS and ABDS patients have partial or complete absence of the abducens nucleus and nerve bilaterally. Differences in residual

adduction and the presence of mild abduction in two patients imply variable depletion of abducens motoneurons and interneurons. Similarly, variable dysinnervation of the lateral rectus by branches of the oculomotor nerve may explain differences in globe retraction and fissure narrowing on both voluntary adduction and convergence.

Surprisingly, brain neuroimaging is relatively normal in BSAS. The brainstem has a normal contour, implying that loss of tissue volume is minimal compared to *Hoxa1* mutations in the mouse, which cause loss of rhombomere 5 and a 40% reduction in the size of the ventral pons.¹⁸ Extraocular muscles appear normal at the resolution of available images, suggesting that the lateral rectus muscle received sufficient innervation for myofiber survival. The supratentorial brain also has a normal appearance despite autism in two patients with BSAS and mental retardation in all patients with ABDS. Only patients with ABDS severely affected by central hypoventilation were reported to have diffuse cortical atrophy, possibly secondary to recurrent hypoxia.⁴

Deafness is arguably the most important disability in patients with BSAS. The eight deaf patients with BSAS all had the common cavity deformity and underdeveloped petrous bones. *Hoxa1*^{-/-} mice also have variable developmental abnormalities in the inner,^{17,19} middle,^{2,17} and external ear² even though *Hoxa1* expression has not been reported in the otic vesicle. Inductive signals from the adjacent hindbrain neuroectoderm and notochord are necessary for otic vesicle patterning,^{20,21} and hindbrain defects associated with *Hoxa1*/*HOXA1* dysfunction may lead to inner ear malformations. Current patients with BSAS were enrolled primarily because of visual abnormalities, and the prevalence of *HOXA1* abnormalities in deafness clinics is not yet known.

All six patients with BSAS studied appropriately had cerebrovascular malformations, and the majority of patients with ABDS had conotruncal heart defects.⁴ Carotid arteries and cardiac out-flow tract arise from symmetrically paired dorsal aortae, aortic arches, and the aortic sac, which appear in the third and fourth weeks of gestation.²² *Hoxa1* is expressed in lateral plate and paraxial mesoderm as vasculogenesis commences in the mouse²³ and could regulate aspects of angioblast migration or remodeling of primordial aortic arch vessels,²⁴ a process dependent upon neural crest cells and lateral plate mesoderm.^{25,26} Vascular defects in these patients with BSAS were clinically silent but probably place patients at increased risk of cerebrovascular compromise.

Two patients with BSAS had autism spectrum disorder and another had autistic features. These observations are surprising because the CNS expression pattern of *Hoxa1* in vertebrates has a rostral limit at the boundary of rhombomere 3 and 4 prior to neurogenesis²⁷ and at the midbrain-forebrain boundary following neurogenesis.²⁸ Loss of *HOXA1* function might cause cortical and cerebellar abnormalities by disturbing development of serotonergic neurons in the brainstem¹ that may modulate cerebral cortex columnar organization and cerebellar Purkinje cell arborization.^{29,30} The *HOXA1* syndrome implies that correct hindbrain development may be necessary for normal cognition and behavior, and studies of patients with BSAS and ABDS and mutant mice are necessary to determine how *HOXA1*/*Hoxa1* function regulates cognitive and behavioral maturation. Patients with BSAS had relatively large skulls, as reported previously in patients with a *HOXA1* polymorphism.³¹

The constellation of congenital defects in BSAS is similar to abnormalities described in thalidomide exposure between 20 and 24 days post-fertilization.^{32,33} These thalidomide children sometimes manifest DRS, facial nerve palsy, deafness, external ear anomalies, other somatic abnormalities, autism, and mental retardation, suggesting that thalidomide may disrupt early rhombomere development,³⁴ possibly by a direct effect on *HOXA1* or downstream pathways.

Supplementary Material

Refer to Web version on PubMed Central for supplementary material.

Acknowledgments

The authors thank the participants in this study.

Supported in part by NIH-RO1-EY015298 (E.C.E.).

GLOSSARY

ABDS	Athabaskan brainstem dysgenesis syndrome
BSAS	Bosley-Salih-Alorainy syndrome
CARS	Childhood Autism Rating Scale
CCA	common carotid artery
CCD	common cavity deformity
CN	cranial nerve
C-spine	cervical spine
DRS	Duane retraction syndrome
DSM-4	Diagnostic and Statistical Manual of Mental Disorders
ET	esotropia
IAC	internal auditory canal
ICA	internal carotid artery
MRA	magnetic resonance angiography
NA	not available
OD	right eye
ortho	orthophoria
OS	left eye
OU	both eyes
PCom	posterior communicating artery
TOF	time-of-flight
US	ultrasound
VAB	Vineland Adaptive Behavior
WNL	within normal limits
XT	exotropia

REFERENCES

1. Tischfield MA, Bosley TM, Salih MA, et al. Homozygous HOXA1 mutations disrupt human brainstem, inner ear, cardiovascular and cognitive development. *Nat Genet* 2005;37:1035–1037. [PubMed: 16155570]

2. Chisaka O, Musci TS, Capecchi MR. Developmental defects of the ear, cranial nerves and hindbrain resulting from targeted disruption of the mouse homeobox gene *Hox-1.6*. *Nature* 1992;355:516–520. [PubMed: 1346922]
3. Lufkin T, Dierich A, LeMeur M, Mark M, Chambon P. Disruption of the *Hox-1.6* homeobox gene results in defects in a region corresponding to its rostral domain of expression. *Cell* 1991;66:1105–1119. [PubMed: 1680563]
4. Holve S, Friedman B, Hoyme HE, et al. Athabaskan brainstem dysgenesis syndrome. *Am J Med Genet A* 2003;120:169–173. [PubMed: 1283395]
5. Jen JC, Chan WM, Bosley TM, et al. Mutations in a human *ROBO* gene disrupt hindbrain axon pathway crossing and morphogenesis. *Science* 2004;304:1509–1513. [PubMed: 15105459]
6. Bosley TM, Salih MA, Jen JC, et al. Neurologic features of horizontal gaze palsy and progressive scoliosis with mutations in *ROBO3*. *Neurology* 2005;64:1196–1203. [PubMed: 15824346]
7. Evans JC, Frayling TM, Ellard S, Gutowski NJ. Confirmation of linkage of Duane's syndrome and refinement of the disease locus to an 8.8-cM interval on chromosome 2q31. *Hum Genet* 2000;106:636–638. [PubMed: 10942112]
8. Demer J, Clark RA, Lim K-H, Engle EC. Magnetic resonance imaging evidence for widespread orbital dysinnervation in dominant Duane's retraction syndrome linked to the *DURS2* locus. *IOVS* 2007;48:194–202.
9. Chung M, Stout JT, Borchert MS. Clinical diversity of hereditary Duane's retraction syndrome. *Ophthalmology* 2000;107:500–503. [PubMed: 10711888]
10. Appukuttan B, Gillanders E, Juo SH, et al. Localization of a gene for Duane retraction syndrome to chromosome 2q31. *Am J Hum Genet* 1999;65:1639–1646. [PubMed: 10577917]
11. Engle EC, Andrews C, Law K, Demer JL. Two pedigrees segregating Duane's retraction syndrome as a dominant trait map to the *DURS2* genetic locus. *Invest Ophthalmol Vis Sci* 2007;48:189–193. [PubMed: 17197532]
12. Al-Baradie R, Yamada K, Hilaire C, et al. Duane radial ray syndrome (Okhiro syndrome) maps to 20q13 and results from mutations in *SALL4*, a new member of the *SAL* family. *Am J Hum Genet* 2002;71:1195–1199. [PubMed: 12395297]
13. Miller NR, Kiel SM, Green WR, Clark AW. Unilateral Duane's retraction syndrome (Type 1). *Arch Ophthalmol* 1982;100:1468–1472. [PubMed: 7115176]
14. Scott AB, Wong GY. Duane's syndrome. An electro-myographic study. *Arch Ophthalmol* 1972;87:140–147. [PubMed: 5057862]
15. Papst W, Esslen E. Symptomatology and therapy in ocular motility disturbances. *Am J Ophthalmol* 1964;58:275–291. [PubMed: 14202515]
16. Hotchkiss MG, Miller NR, Clark AW, Green WR. Bilateral Duane's retraction syndrome. A clinical-pathologic case report. *Arch Ophthalmol* 1980;98:870–874. [PubMed: 7378011]
17. Mark M, Lufkin T, Vonesch JL, et al. Two rhombomeres are altered in *Hoxa-1* mutant mice. *Development* 1993;119:319–338. [PubMed: 8287791]
18. del Toro ED, Borday V, Davenne M, Neun R, Rijli FM, Champagnat J. Generation of a novel functional neuronal circuit in *Hoxa1* mutant mice. *J Neurosci* 2001;21:5637–5642. [PubMed: 11466434]
19. Gavalas A, Studer M, Lumsden A, Rijli FM, Krumlauf R, Chambon P. *Hoxa1* and *Hoxb1* synergize in patterning the hindbrain, cranial nerves and second pharyngeal arch. *Development* 1998;125:1123–1136. [PubMed: 9463359]
20. Bok J, Bronner-Fraser M, Wu DK. Role of the hind-brain in dorsoventral but not anteroposterior axial specification of the inner ear. *Development* 2005;132:2115–2124. [PubMed: 15788455]
21. Barald KF, Kelley MW. From placode to polarization: new tunes in inner ear development. *Development* 2004;131:4119–4130. [PubMed: 15319325]
22. Larsen, WJ. *Human embryology*. 3rd ed.. Churchill Livingstone; 2001.
23. Murphy P, Hill RE. Expression of the mouse labial-like homeobox-containing genes, *Hox 2.9* and *Hox 1.6*, during segmentation of the hindbrain. *Development* 1991;111:61–74. [PubMed: 1673098]
24. Risau W. Mechanisms of angiogenesis. *Nature* 1997;386:671–674. [PubMed: 9109485]

25. Etchevers HC, Vincent C, Le Douarin NM, Couly GF. The cephalic neural crest provides pericytes and smooth muscle cells to all blood vessels of the face and forebrain. *Development* 2001;128:1059–1068. [PubMed: 11245571]
26. Wang W, Grimmer JF, Van De Water TR, Lufkin T. Hmx2 and Hmx3 homeobox genes direct development of the murine inner ear and hypothalamus and can be functionally replaced by *Drosophila* Hmx. *Dev Cell* 2004;7:439–453. [PubMed: 15363417]
27. Carpenter E, Goddard J, Chisaka O, Manley N, Capecchi M. Loss of Hox-A1 (Hox-1.6) function results in the reorganization of the murine hindbrain. *Development* 1993;118:1063–1075. [PubMed: 7903632]
28. McClintock JM, Jozefowicz C, Assimacopoulos S, Grove EA, Louvi A, Prince VE. Conserved expression of Hoxa1 in neurons at the ventral forebrain/midbrain boundary of vertebrates. *Dev Genes Evol* 2003;213:399–406. [PubMed: 12748854]
29. Janusonis S, Gluncic V, Rakic P. Early serotonergic projections to Cajal-Retzius cells: relevance for cortical development. *J Neurosci* 2004;24:1652–1659. [PubMed: 14973240]
30. Kondoh M, Shiga T, Okado N. Regulation of dendrite formation of Purkinje cells by serotonin through serotonin1A and serotonin2A receptors in culture. *Neurosci Res* 2004;48:101–109. [PubMed: 14687886]
31. Conciatori M, Stodgell CJ, Hyman SL, et al. Association between the HOXA1 A218G polymorphism and increased head circumference in patients with autism. *Biol Psychiatry* 2004;55:413–419. [PubMed: 14960295]
32. Miller MT. Thalidomide embryopathy: a model for the study of congenital incontinent horizontal strabismus. *Trans Am Ophthalmol Soc* 1991;89:623–674. [PubMed: 1808819]
33. Stromland K, Miller MT. Thalidomide embryopathy: revisited 27 years later. *Acta Ophthalmol (Copenh)* 1993;71:238–245. [PubMed: 8333272]
34. Miller MT, Stromland K. The Möbius sequence: a re-look. *JAAPOS* 1999;3:199–208.

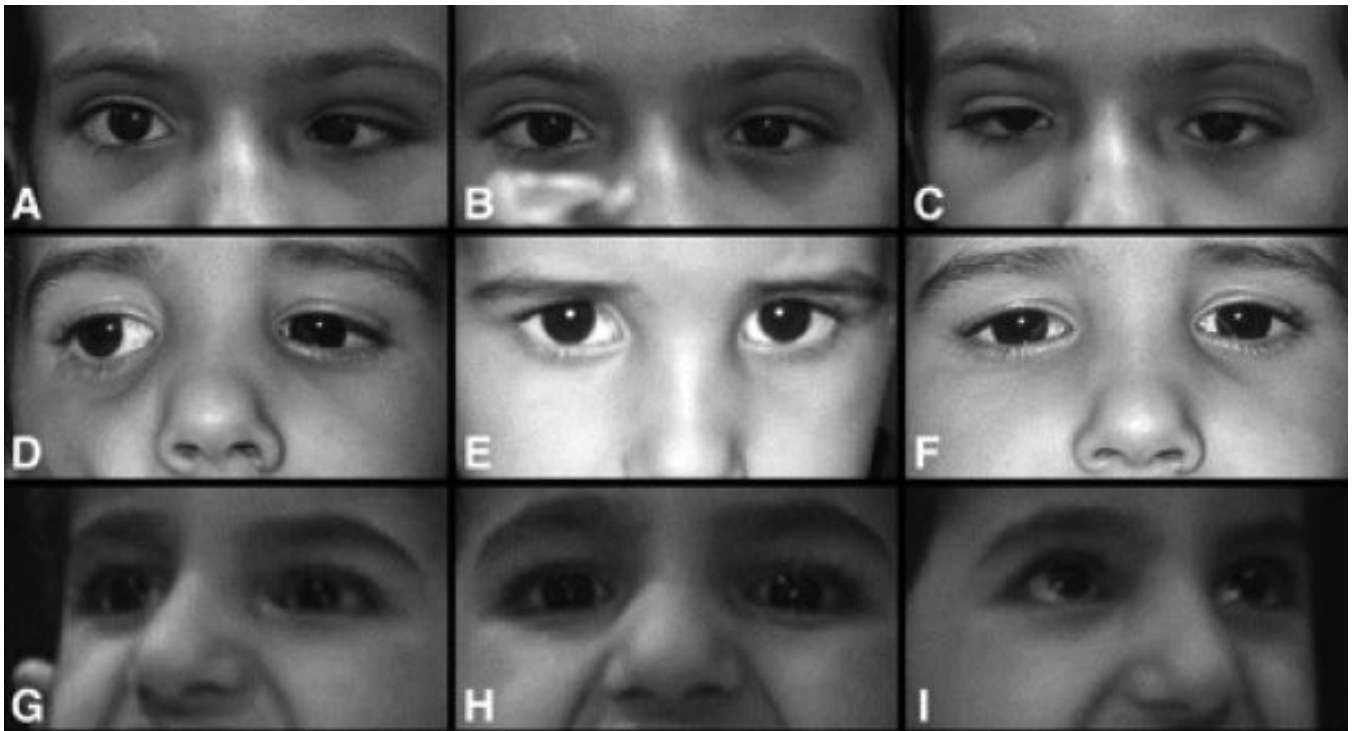


Figure 1. Variability of ocular alignment and motility

Images A, D, and G are right gaze, while images B, E, and H are in primary position, and images C, F, and I are left gaze. Top row (A, B, and C) are of Patient 4 who had a primary position esotropia with no anomalous head position when fixing with the right eye. This patient was unable to abduct either eye beyond the midline but demonstrated modest adduction bilaterally with globe retraction and fissure narrowing of the adducting eye. Middle row (D, E, and F) are of Patient 8 who was orthotropic in primary position but adopted a small face turn left to maintain comfortable binocular fixation. He had no eye movements to the left but modest symmetric movement of both eyes into right gaze. Bottom row (G, H, and I) are of Patient 5, who was orthotropic in primary position and had severely limited eye movements bilaterally with only minimal adduction the right eye. No abnormal head posture was present in primary position but she used a face turn to view objects to the right or left.

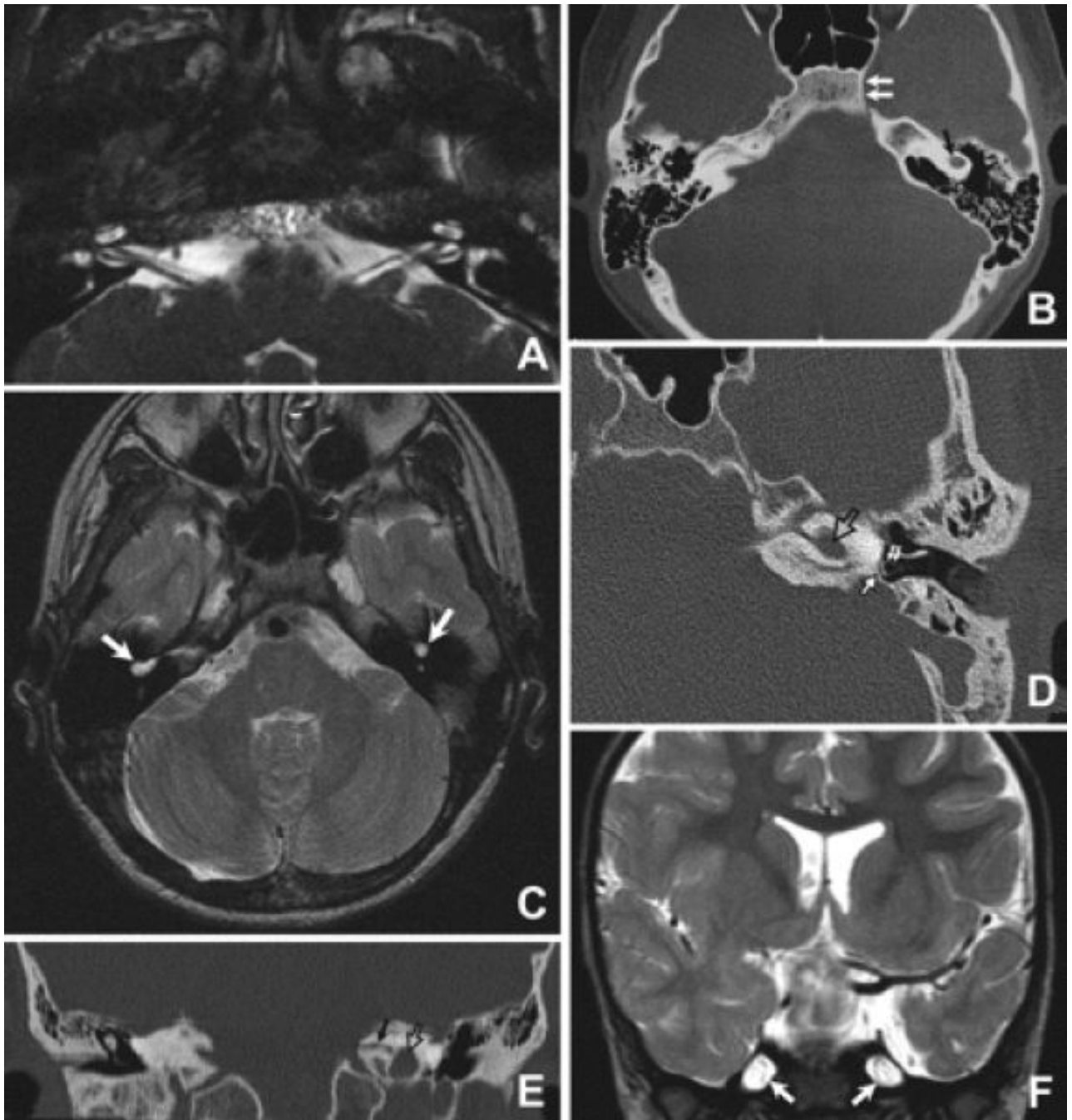


Figure 2. Variability of skull base neuroimaging

(A) High resolution axial constructive interference in steady-state MR image of the inner ear and low brainstem of Patient 8 demonstrating normal inner ear structures and normal lower cranial nerves. (B, C) Axial CT (B) and T2-weighted MR images (C) at the level of the inner ear of Patient 6 demonstrating bilateral common cavity deformity (black arrow in B and white arrows in C). The medial part of the left carotid canal is absent (double arrows in B) while the right one is present. (D) Axial CT of the petrous bone of Patient 3 showing common cavity deformity of the left inner ear (open arrow) with normal stapes (double arrows) and lack of development of the oval window opposite to the footplate of stapes (solid arrow). (E) Reconstructed coronal CT image of the petrous bone of Patient 3 showing the common cavity

deformity of the left inner ear (open arrow) and severe stenosis of the left internal auditory canal (black arrow). Inner ear structures on the right side are absent. (F) Coronal T2-weighted MR image of Patient 7 showing patulous Meckle's caves (arrows).

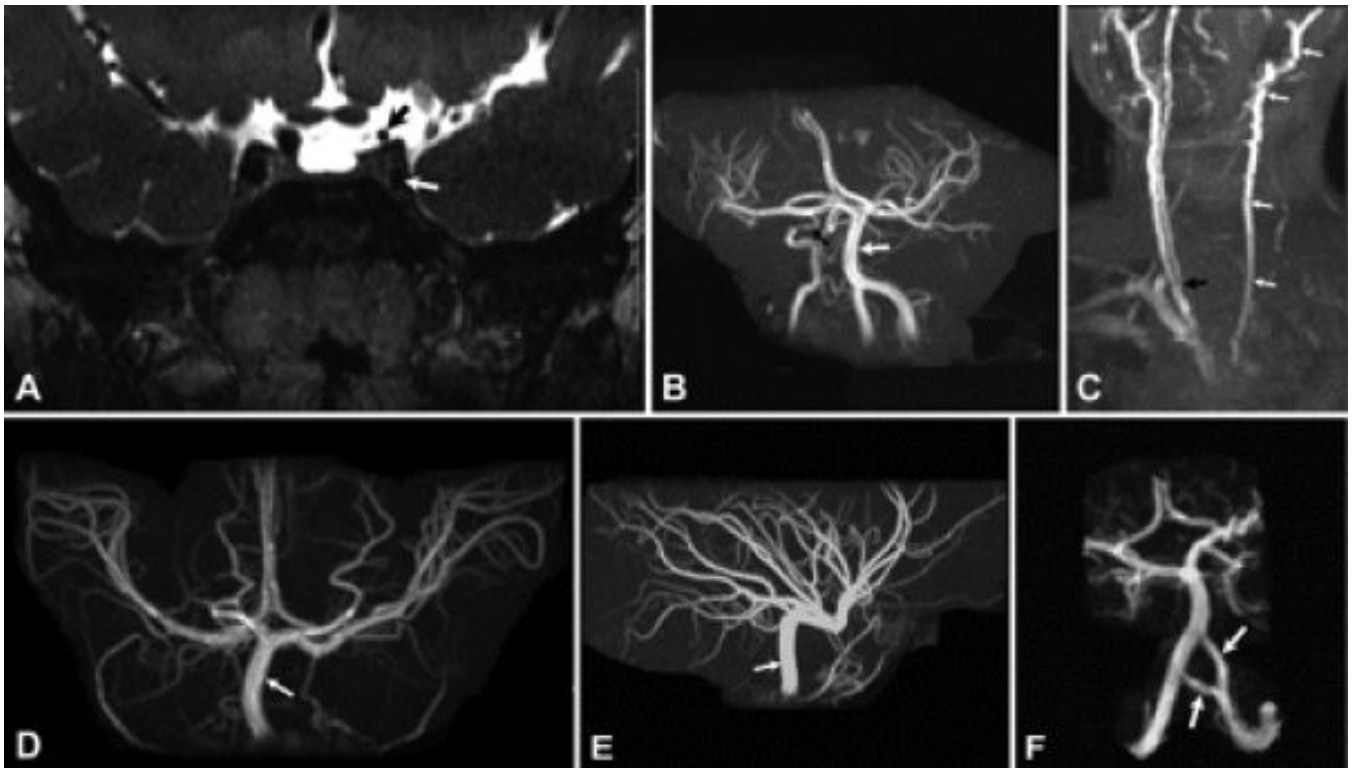


Figure 3. Variability of MR angiography

(A) Coronal T2-weighted MR image of Patient 8 demonstrating hypoplasia of the cavernous (white arrow) and supraclinoid (black arrow) portions of the left internal carotid artery. The cavernous and supraclinoid portions of the right internal carotid artery have normal caliber. (B) MR angiogram of the brain of Patient 6 showing absence of the left internal carotid artery and hypoplasia of the cavernous portion of the right internal carotid artery (black arrow). Vertebral and basilar arteries (white arrow) have larger caliber than the right internal carotid artery. (C) MR angiogram of the neck of Patient 6 demonstrating absence of the left internal carotid artery with the common carotid artery ending as a continuation of external carotid artery (white arrows). The right common carotid artery has a bifurcation (black arrow) at about the level of the C7 vertebra, while normal bifurcation of common carotid artery is about the level of C4. (D, E) Anterior (D) and lateral (E) projections of the MR angiogram of the brain of Patient 5 demonstrating absence of both internal carotid arteries and enlargement of the basilar (arrow) and posterior communicating arteries, which supply both the anterior and posterior cerebral circulations. (F) MR angiogram of the brain of Patient 5 showing duplication of the intracranial portion of the left vertebral artery (arrows).

Table 1

General information

Patient	Family	Age, y	Sex	Deaf	Motor milestones	Autistic spectrum disorder	Other
1	KF	17	F	Yes	WNL	No	Flattened ear helix bilaterally
2	KF	5	M	Yes	Delayed	No	Polydactyly of left foot; brachydactyly of 4th and 5th toes; duplex ureteral system with urethral stricture
3	KF	20	M	Yes	Walking by 4 y	Yes	Smaller right side of face; flattened ear helix bilaterally; frequent grimacing
4	LF	11	F	Yes	Delayed	No	Recurrent choking until age 1½ years
5	LF	4	F	Yes	Not sitting or crawling by 4 y	Yes	Chronic constipation; sleep disturbance; low amplitude horizontal pendular nystagmus
6	LG	18	F	Yes	Walking by 3 y	No	Low amplitude vertical pendular nystagmus
7	LG	4	F	Yes	Walking by 3 y; still unsteady at 4 y	No	Chronic constipation; low positioned ears with anteriorly angulated right auricle; frequent grimacing
8	NO	4	M	No	WNL	No	Right talipes equinovarus repaired surgically
9	KK	3½	F	Yes	WNL	No	Frequent grimacing

Age = age at last examination; WNL = within normal limits.

Table 2

Ocular motility

Patient	Abduction	Adduction	Globe retraction	Alignment	Convergence	Vertical anomalies
1	30% OU	70% OU	Moderate OU	Moderate ET at distance; near NA	NA	None
2	0% OU	40% OU	Mild OU	Moderate ET at distance and near	Poor	Upshoot OS on left and right gaze when fixing with OD
3	0% OU	30% OU	None observed	Ortho at distance, small XT at near	Absent (poor coop)	None
4	0% OU	60% OD, 70% OS	Marked OU	Small ET at distance and near	Good*	Upshoot on adduction OU; upshoot OD on abduction when fixing with OS
5	0% OU	0% OU	None observed	Ortho	Poor	NA
6[†]	0% OU	60% OU	Moderate OU	Moderate ET at distance; small ET at near	NA	Upshoot in abduction and adduction of nonfixing eye
7	0% OU	10% OD, 0% OS	Moderate OD	Ortho	Poor	None
8	40% OD, 0% OS	0% OD, 40% OS	Moderate OU	Ortho (with left face turn)	Good*	None
9	0% OU	45% OD, 75% OS	Mild OU	Ortho	Moderate*	None

Abduction and adduction expressed in % of normal excursion.

OU = both eyes; ET = esotropia; NA = not available; OS = left eye; OD = right eye; XT = exotropia; ortho = orthophoria; coop = cooperation.

* Globe retraction present OU during convergence.

[†] Patient 6 = preoperative observations

Table 3

Neuroimaging

Patient	Examinations available	Inner ear	Cerebral vasculature	Other
1	CT temporal bones; MRI brain; MRA brain and neck	Right CCD with IAC stenosis; absent left inner ear structures and IAC	Low right CCA bifurcation; hypoplastic left ICA with larger left PCom; duplication of proximal half of left vertebral artery	
2	NA			
3	CT temporal bones	Left CCD with IAC stenosis; absent right inner ear structures and IAC	NA	Small right carotid canal
4	CT temporal bones; MRI brain; MRA brain and neck; US abdomen	Bilateral CCD with bilateral IAC stenosis	Absent left ICA; hypoplastic intracavernous right ICA; low right CCA bifurcation; large basilar system	Absent left carotid canal; normal C-spine
5	CT temporal bones; MRI brain; MRA brain and neck; US abdomen	Bilateral CCD with bilateral absent IAC	Bilateral absent ICAs; large basilar system; duplication of intracranial left vertebral artery	Absent carotid canals bilaterally; normal C-spine
6	CT temporal bones; MRI brain; MRA brain and neck	Bilateral CCD with bilateral IAC stenosis	Absent left ICA; low right CCA bifurcation; hypoplastic intracavernous right ICA; large basilar system	Absent left carotid canal; normal C-spine
7	CT brain; MRI brain; MRA brain; US abdomen	Bilateral CCD with bilateral absent IAC	Absent left ICA; low right CCA bifurcation; large basilar system	Normal C-spine
8	MRI brain	Normal inner ear bilaterally	Hypoplastic left ICA; large left PCom	CN 6 not conclusively visible bilaterally
9	NA			

Columns 3 and 4 modified from Tischfield et al.,¹ Supplementary Table 1 Online.

MRA = magnetic resonance angiography; CCD = common cavity deformity; IAC = internal auditory canal; CCA = common carotid artery; ICA = internal carotid artery; PCom = posterior communicating artery; NA = not available; C-spine = cervical spine; US = ultrasound.